Dalton Transactions

Cite this: *Dalton Trans.*, 2011, **40**, 7423

www.rsc.org/dalton

PAPER

Aluminium complexes containing bidentate and symmetrical tridentate pincer type pyrrolyl ligands: synthesis, reactions and ring opening polymerization†

Wen-Yen Huang,[a] Sheng-Jie Chuang,[a] Nien-Tsu Chunag,[a] Ching-Sheng Hsiao,[a] Amitabha Datta,[a] Shau-Jiun Chen,[a] Ching-Han Hu,[a] Jui-Hsien Huang,*[a] Ting-Yu Lee[b] and Chia-Her Lin[c]

Received 16th March 2011, Accepted 6th May 2011
DOI: 10.1039/c1dt10442j

A series of aluminium derivatives containing substituted bidentate and symmetrical tridentate pyrrolyl ligands, $[C_4H_3NH(2\text{-}CH_2NH^tBu)]$ and $[C_4H_2NH(2,5\text{-}CH_2NH^tBu)_2]$, in toluene or diethyl ether were synthesized. Their reactivity and application for the ring opening polymerization of ε-caprolactone have been investigated. The reaction of $AlMe_3$ with one equiv. of $[C_4H_3NH(2\text{-}CH_2NH^tBu)]$ in toluene at room temperature affords $[C_4H_3N(2\text{-}CH_2NH^tBu)]AlMe_2$ (**1**) in 70% yield by elimination of one equiv. of methane. Interestingly, while reacting $AlMe_3$ with one equiv. of $[C_4H_3NH(2\text{-}CH_2NH^tBu)]$ in toluene at 0 °C followed by refluxing at 100 °C, $[\{C_4H_3N(2\text{-}CH_2N^tBu)\}AlMe]_2$ (**2**) has been isolated *via* fractional recrystalliztion in 30% yield. Similarly, reacting $AlMe_3$ with two equiv. of $C_4H_3NH(2\text{-}CH_2NH^tBu)$ generates $[C_4H_3N(2\text{-}CH_2NH^tBu)]_2AlMe$ (**3**) in a moderate yield. Furthermore, complex **1** can be transformed to an aluminium alkoxide derivative, $[C_4H_3N(2\text{-}CH_2NH^tBu)][OC_6H_2(\text{-}2,6\text{-}^tBu_2\text{-}4\text{-}Me)]AlMe$ (**4**) by reacting **1** with one equiv. of $HOC_6H_2(\text{-}2,6\text{-}^tBu_2\text{-}4\text{-}Me)$ in toluene *via* the elimination of one equiv. of methane. The reaction of AlR_3 with one equiv. of $[C_4H_2NH(2,5\text{-}CH_2NH^tBu)_2]$ in toluene at room temperature affords $[C_4H_2N(2,5\text{-}CH_2NH^tBu)_2]AlR_2$ (**5**, R = Me; **6**, R = Et) in moderate yield. Surprisingly, from the reaction of two equiv. of $[C_4H_2NH(2,5\text{-}CH_2NH^tBu)_2]$ with $LiAlH_4$ in diethyl ether at 0 °C, a novel complex, $[C_4H_2N(2\text{-}CH_2N^tBu)(5\text{-}CH_2NH^tBu)]_2AlLi$ (**7**) has been isolated after repeating re-crystallization. Furthermore, reacting one equiv. of $C_4H_2NH(2,5\text{-}CH_2NH^tBu)_2$ with $AlH_3{\cdot}NMe_3$ in diethyl ether generates an aluminium dihydride complex, $[C_4H_2N(2,5\text{-}CH_2NH^tBu)_2]\text{-}AlH_2$ (**8**), in high yield. Additionally, treating **8** with one equiv. of $HOC_6H_2(\text{-}2,6\text{-}^tBu_2\text{-}4\text{-}Me)$ in methylene chloride produces $[C_4H_2N(2,5\text{-}CH_2NH^tBu)_2][OC_6H_2(\text{-}2,6\text{-}^tBu_2\text{-}4\text{-}Me)]AlH$ (**9**) with the elimination of one equiv. of H_2. The aluminium alkoxide complex **4** shows moderate reactivity toward the ring opening polymerization of ε-caprolatone in toluene.

Introduction

Aluminium alkyl[1] and aluminium hydride[2] complexes supported by various types of ligands have been extensively investigated and reviewed in the past decades due to their potential usages such as synthesizing (1) aluminium cation complexes[3] as catalysts for olefin polymerization, (2) aluminium alkoxide complexes[4] as initiators for ring opening polymerization of lactones and lactides, (3) alkylalumoxanes[5] as co-catalysts for olefin polymerization, (4) reducing agents[6] in organic synthesis and (5) hydrogen storage materials.[7] The reactions of aluminium alkyl or hydride complexes involve deprotonation, insertion, and abstraction as shown in Scheme 1.

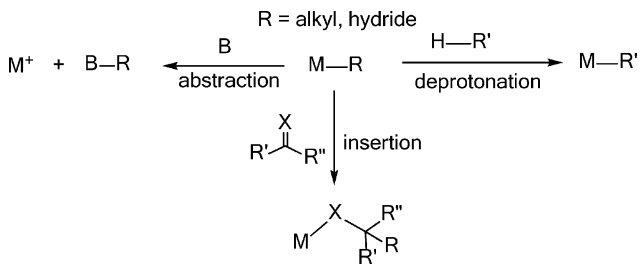

Scheme 1

Concerning different ligand systems, the pyrrolyl entity has the capability to bring metal atoms into close proximity and

[a]*Department of Chemistry, National Changhua University of Education, Changhua, Taiwan, 500*
[b]*Department of Applied Chemistry, National Kaohsiung University, Kaohsiung, Taiwan, 500*
[c]*Department of Chemistry, Chung-Yuan Christian University, Chung-Li 320, Taiwan. E-mail: juihuang@cc.ncue.edu.tw*

† Electronic supplementary information (ESI) available: NMR spectra of complex **7** and Crystal data and structure refinement for complex **2** (second set of crystal data). CCDC reference numbers 792978–792982 and 808790–808793. For ESI and crystallographic data in CIF or other electronic format see DOI: 10.1039/c1dt10442j

provides an intramolecular or intermolecular pathway for bonding interactions. Substituted pyrrole heterocycles also show important biological activity. For example, various substituted pyrroles are known to act as analgesics, anti-inflammatory agents, or to have antibacterial properties.[8] However, relatively few metal–pyrrole complexes have been found to be synthetically useful in the preparation of substituted pyrrole rings, and the syntheses of substituted pyrroles have been largely limited to electrophilic additions to the free ligand and to ring-closing reactions of appropriate precursors.[9] To summarize the chemistry of the pyrrolyl based system, the reactions of aluminium hydride complexes with ketones generate aluminium alkoxide complexes[10] and we also showed the reactivity of monomeric aluminium hydride complexes with pyrrolyl ligands[11] reflecting insertion and the C–C coupling mechanistic pathway. The role of organoaluminium hydrides in facilitating the reactions of donor-substituted pyrrole ligands with PhNCO, CO_2, H_2O, and tertiary alcohols have been recognized[12] but considerable work remains to establish a thorough understanding of metal coordination effects on pyrrole reactivity as nitrogen based polydentate ancillary ligands.

We have been investigating the development of non-toxic metal complexes as initiators for the lactone ring opening polymerization in the past years using substituted pyrrole as supporting ligands.[13] As an extension of our continuous interest in the pyrrolyl ligand system, the present contribution focuses on the synthesis, characterization and reactivity study of aluminium complexes using bidentate and symmetric tridentate pincer type pyrrolyl ligands. In addition, complex **4** can participate in the ring-opening polymerization of ε-caprolactone, acting as a catalyst.

Results and discussion

Syntheses and characterization of complexes 1–9

The reactions of $AlMe_3$ with $C_4H_3NH(2\text{-}CH_2NH^tBu)$ are shown in Scheme 2. The reaction of $AlMe_3$ with $[C_4H_3NH(2\text{-}CH_2NH^tBu)]$ in toluene at room temperature affords a four-coordinate aluminium dimethyl complex $[C_4H_3N(2\text{-}CH_2NH^tBu)]AlMe_2$ (**1**) in 70% yield along with the elimination of one equiv. of methane. The ^1H and ^{13}C NMR spectra of the methyl groups of Al*Me*$_2$ show a singlet at δ –0.28 and a broad signal at δ –7.8, respectively. The broad ^{13}C NMR resonance is resulting from the quadruple interaction of Al atoms (I = 5/2).[14] The methylene protons of C*H*$_2$NH^{t}Bu show two doublets at δ 3.40. Alternatively, while reacting $AlMe_3$ with $[C_4H_3NH(2\text{-}CH_2NH^tBu)]$ in toluene at 0 °C followed by heating at 93 °C, complex **1** and the dimeric aluminium complex $[\{C_4H_3N(2\text{-}CH_2N^tBu)\}AlMe]_2$ (**2**) were both obtained and **2** can be isolated *via* fractional recrystalliztion in 30% yield. The ^1H NMR spectrum of **2** shows a singlet at δ –0.17 for the methyl protons of the Al*Me* and two doublets at δ 3.83 and 4.21 for the methylene protons of C*H*$_2$N^{t}Bu. No amino proton resonance of N*H*^{t}Bu was observed for **2**, although it appeared at δ 2.13 for **1**. Complex **1** is quite thermally stable, which remains unchanged while heating at 110 °C for 12 h. This phenomenon demonstrates that the mechanistic pathway does not proceed through **1** during the formation of **2** from a combination of $AlMe_3$ and $C_4H_3NH(2\text{-}CH_2NH^tBu)$. Possible reaction mechanisms for the formation of complexes **1** and **2** are shown in Scheme 3 where $AlMe_3$ might have a better chance to bind to the acidic protons of the pyrrole and amine simultaneously at low temperature to generate the dimeric complex **2**.

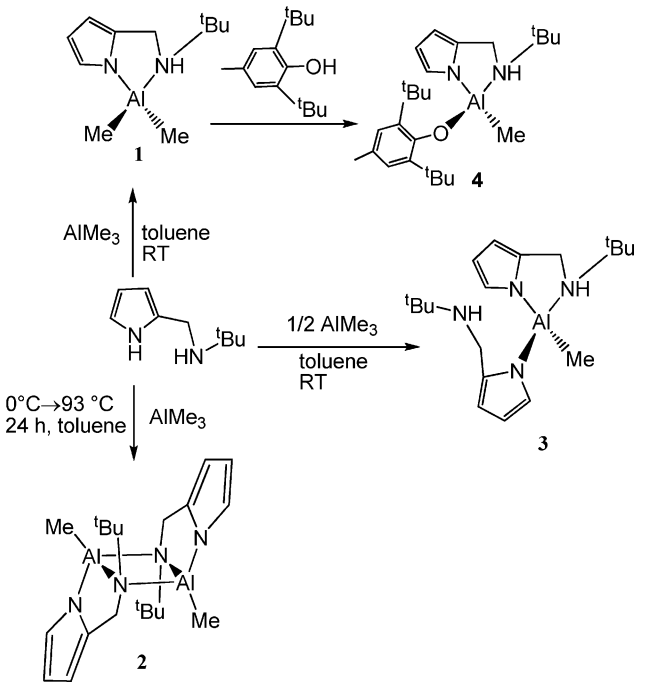

Scheme 2

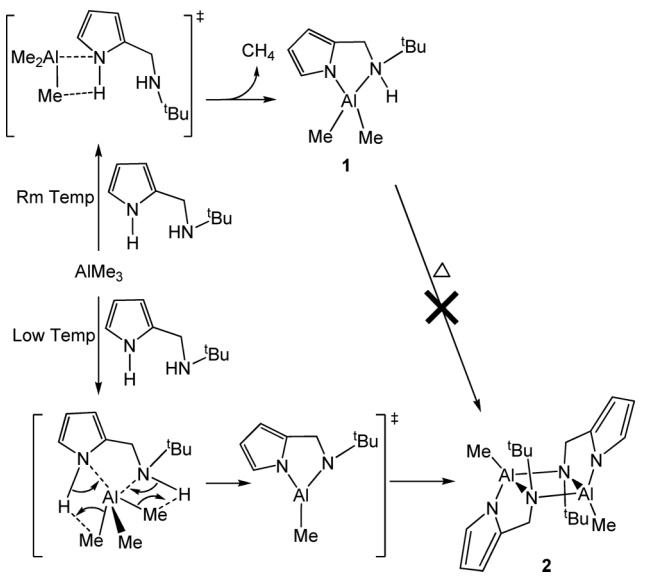

Scheme 3

Similarly, reacting $AlMe_3$ with two equiv. of $C_4H_3NH(2\text{-}CH_2NH^tBu)$ affords a four-coordinate aluminium methyl complex $[C_4H_3N(2\text{-}CH_2NH^tBu)]_2AlMe$ (**3**). The ^1H NMR spectra of **3** at room temperature show a singlet at δ –0.17 for the methyl protons of the Al*Me* and two doublets at δ 3.44 appearing as a broad band for the methylene protons of C*H*$_2$NH^{t}Bu. A small broad band is observed at δ 3.83, which is assigned as the amino proton of N*H*^{t}Bu. Variable temperature ^1H NMR spectra of **3** in d^8-toluene were obtained ranging from 213~343 K showing no significant changes for the ^1H NMR resonances. This phenomenon indicates

a fast exchange happened between the two substituted pyrrolyl ligands bonding to the Al atom as shown in Scheme 4.

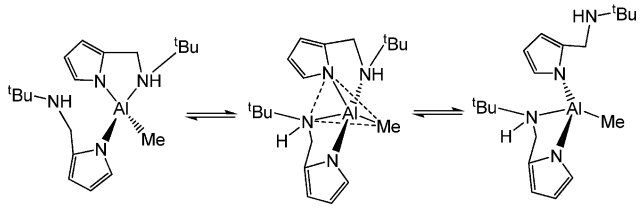

Scheme 4

Complex **1** can be converted to the aluminium alkoxide complex $[C_4H_3N(2\text{-}CH_2NH^tBu)][OC_6H_2(\text{-}2,6\text{-}^tBu_2\text{-}4\text{-}Me)]AlMe$ (**4**) by reacting **1** with one equiv. of $HOC_6H_2(\text{-}2,6\text{-}^tBu_2\text{-}4\text{-}Me)$ in toluene along with the elimination of one equiv. of methane (Scheme 2). On the addition of excess alcohol, no further methane elimination was observed, an indication of the large sterically crowded alkoxide ligand blocking the pathway of a second alcohol into penetration with the aluminium methyl fragment. The ^1H and ^{13}C NMR spectra of **4** show a singlet at δ –0.09 and –7.0, respectively, proving the existence of the aluminium methyl.

The reactions of $[C_4H_2NH(2,5\text{-}CH_2NH^tBu)_2]$ with AlR_3, $LiAlH_4$ and alane and its corresponding derivative with $HOC_6H_2(2,6\text{-}^tBu_2\text{-}4\text{-}Me)$ are shown in Scheme 5. The pincer type[15] tri-dentate ligand, $C_4H_2NH(2,5\text{-}CH_2NH^tBu)_2$ was obtained following a similar procedure as for synthesizing the bidentate pyrrolyl ligand $C_4H_3NH(2\text{-}CH_2NH^tBu)$.[16] Reacting $C_4H_2NH(2,5\text{-}CH_2NH^tBu)_2$ with one equiv. of $AlMe_3$ in toluene affords complex **5**, $[C_4H_2N(2,5\text{-}CH_2NH^tBu)_2]AlMe_2$, in 67% yield along with the elimination of one equiv. of methane. Complex **5** was characterized by ^1H and ^{13}C NMR spectra. The chemical shift of the amino proton of CH_2NH^tBu appears at δ 1.59, which shifts slightly depending upon the concentration of the complex in D-solvent due to hydrogen bonding. The methylene protons of CH_2NH^tBu show two doublets of doublets at δ 3.62 and 3.65 while showing different diastereomericity with the $^2J_{HH}$ coupling constant of 8.4 Hz. The ^1H and ^{13}C NMR spectra of the aluminium methyl groups show one singlet at δ –0.31 and –4.9, respectively, representing the strong electronic shielding properties of the anionic alkyl groups. Similarly, complex **6**, $[C_4H_2N(2,5\text{-}CH_2NH^tBu)_2]AlEt_2$, can be obtained from the reaction of $C_4H_2NH(2,5\text{-}CH_2NH^tBu)_2$ with one equiv. of $AlEt_3$ in toluene. The ^1H and ^{13}C NMR spectra of **6** are consistent, similarly to those of complex **5** and no further discussion has been included here.

While $LiAlH_4$ was reacting with one equiv. of $C_4H_2NH(2,5\text{-}CH_2NH^tBu)_2$ in diethyl ether at 0 °C, the evolution of hydrogen gas was observed and a dinuclear complex **7**, $[C_4H_2N(2\text{-}CH_2N^tBu)(5\text{-}CH_2NH^tBu)]_2AlLi$, was isolated after repeating re-crystallization. It is interesting to note that while $LiAlH_4$ reacted with two equiv. of $C_4H_2NH(2,5\text{-}CH_2NH^tBu)_2$, convoluted products were observed from the ^1H NMR spectra without differentiation of pure complex **7**. The asymmetrical geometry of **7** results in complicated NMR spectra. Detailed assignment of the ^1H-^{13}C HSQC 2D NMR spectra and ^1H-^1H NOESY 2D NMR spectra were provided in the ESI.† In addition, the ν_{NH} stretching frequency appearing at 3248 cm^{-1} indicates that one of the two side arms of the pyrrolyl ligands retains its neutrality of amino functionality.

Reacting one equiv. of $C_4H_2NH(2,5\text{-}CH_2NH^tBu)_2$ with alane, $AlH_3{\cdot}NMe_3$, in diethyl ether and recrystallizing from methylene chloride results in an aluminium dihydride complex **8**, $[C_4H_2N(2,5\text{-}CH_2NH^tBu)_2]AlH_2$, in high yield. A deuterated complex $[C_4H_2N(2,5\text{-}CH_2NH^tBu)_2]AlD_2$ (**8-D**) can also be obtained from $C_4H_2NH(2,5\text{-}CH_2NH^tBu)_2$ and $AlD_3{\cdot}NMe_3$. The IR spectra show that the $\nu_{Al\text{-}H}$ stretching frequency shifted from 1801 to 1318 cm^{-1} for $\nu_{Al\text{-}D}$ (calculated at 1319 cm^{-1}). The ^1H NMR spectra of **8** show a singlet at δ 2.58 to the corresponding amino proton of NH^tBu. Again the methylene protons of CH_2NH^tBu appear as a doublet at δ 3.72, further proving the $^3J_{HH}$ coupling of CH_2 and NH. Treating **8** with one equiv. of $HOC_6H_2(\text{-}2,6\text{-}^tBu_2\text{-}4\text{-}Me)$ in methylene chloride yields $[C_4H_2N(2,5\text{-}CH_2NH^tBu)_2]AlH[OC_6H_2(\text{-}2,6\text{-}^tBu_2\text{-}4\text{-}Me)]$ (**9**) with the elimination of one equiv. of H_2. The ^1H NMR spectra of methylene protons of CH_2NH^tBu appeared as multiplets at δ 3.77 due to the rigidity of the complex geometry arising from the bulky aryloxide substituent. The amino proton of CH_2NH^tBu shows one singlet at δ 2.32, which overlaps with the signal of the methyl group of the aryloxide fragment. The hydride signal was not observed in the ^1H NMR spectra, therefore, a deuterated complex $[C_4H_2N(2,5\text{-}CH_2NH^tBu)_2]AlD[OC_6H_2(\text{-}2,5\text{-}^tBu_2\text{-}4\text{-}Me)]$ (**9-D**) was synthesized

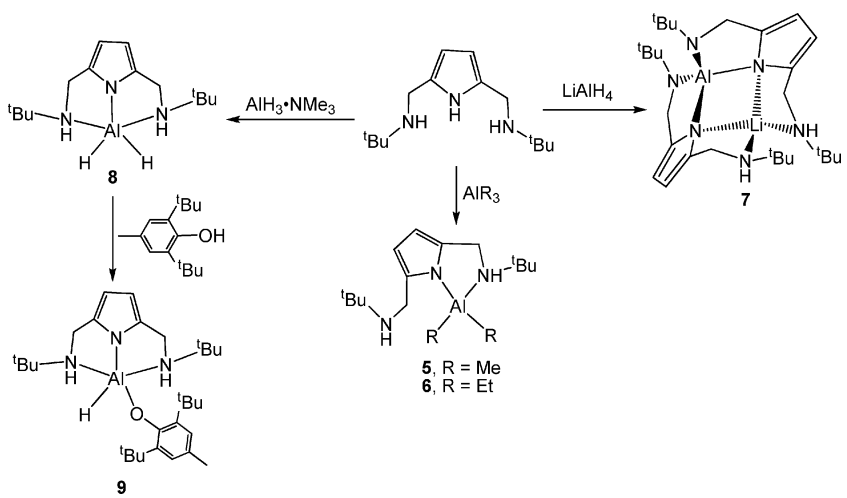

Scheme 5

Table 1 Summary of data collections for complexes **1–7** and **9**

	1	**2**	**3**	**4**	**5**	**6**	**7**	**9**
Formula	$C_{11}H_{21}AlN_2$	$C_{20}H_{34}Al_2N_4$	$C_{19}H_{33}AlN_4$	$C_{25}H_{41}AlN_2O$	$C_{16}H_{32}AlN_3$	$C_{18}H_{36}AlN_3$	$C_{63}H_{108}Al_2Li_2N_{12}$	$C_{29}H_{50}AlN_3O$
FW	208.28	384.47	344.47	412.58	293.43	321.48	1101.45	483.70
Crystal system	Monoclinic	Monoclinic	Monoclinic	Monoclinic	Triclinic	Monoclinic	Monoclinic	Monoclinic
Space group	$P2_1/n$	$C2/c$	$P2_1/c$	$C2/c$	P –1	$P2_1/c$	$P2_1/c$	$P2_1/c$
a/Å	8.0962(3)	10.8437(8)	15.980(3)	24.0326(19)	9.0135(8)	10.4122(7)	9.2957(3)	17.1684(3)
b/Å	12.8293(4)	15.3133(11)	15.156(3)	12.5009(7)	9.9804(9)	17.7071(11)	20.3506(8)	10.1390(2)
c/Å	12.8195(4)	26.1398(19)	17.705(3)	18.4002(16)	10.8491(8)	10.7696(7)	17.9295(6)	16.2407(3)
α/°	90	90	90	90	103.080(5)	90	90	90
β/°	100.424(2)	96.2580(10)	99.467(13)	116.566(7)	96.371(5)	102.188(7)	99.594(2)	92.7340(10)
γ/°	90	90	90	90	102.129(5)	90	90	90
V/Å^3, Z	1309.57(8), 4	4314.7(5), 8	4229.6(14), 8	4944.3(6), 8	916.46(13), 2	1940.8(2), 4	3344.3(2), 2	2823.81(9), 4
D_c/Mg m^{-3}	1.056	1.184	1.082	1.109	1.063	1.100	1.094	1.138
μ/mm^{-1}	0.125	0.146	0.103	0.099	0.107	0.107	0.089	0.097
T/K	150(2)	150(2)	150(2)	150(2)	150(2)	295(2)	150(2)	150(2)
F(000)	456	1664	1504	1808	324	712	1204	1064
no. of reflns collected	10232	16760	29976	19862	11521	8712	50486	48630
no. of ind reflns	3141	5116	10184	5975	4721	4358	8383	6832
R_{int}	0.0236	0.0255	0.1005	0.0437	0.0265	0.0539	0.0389	0.0606
data/restraints/params	3141/0/136	5116/0/243	10184/0/447	5975/0/277	4721/0/189	4358/0/199	8383/3/373	6832/0/323
goodness of fit on F^2	1.103	1.050	0.761	0.937	1.037	0.946	1.106	1.020
R_1 [$I > 2\sigma(I)$]	0.0351	0.0391	0.0527	0.0451,	0.0403	0.0548	0.0528	0.0418
wR_2 [$I > 2\sigma(I)$]	0.0971	0.1072	0.1206	0.1023	0.1041	0.1208	0.1351	0.0943
R_1 (all data)	0.0447	0.0513	0.2024	0.0980	0.0547	0.0945	0.0819	0.0694
wR_2 (all data)	0.1017	0.1131	0.1524	0.1126	0.1136	0.1298	0.1491	0.1086
largest diff peak and hole/e Å^{-3}	0.235 and –0.164	0.291 and –0.246	0.344 and –0.325	0.233 and –0.254	0.271 and –0.253	0.547 and –0.278	0.560 and –0.338	0.305 and –0.270

from **8**-D and HOC_6H_2(-2,5-^{t}Bu$_2$-4-Me). The IR spectra show that the $\nu_{Al\text{-}H}$ stretching frequency shifted from 1852 cm^{-1} to 1352 cm^{-1} for $\nu_{Al\text{-}D}$.

Molecular structures of 1–7 and 9

The crystallographic data for complexes **1–7** and **9** are summarized in Table 1, and selected bond lengths and angles are listed in Table 2. Orange-red crystals of **1** were obtained from a saturated toluene solution at –20 °C and its molecular structure is shown in Fig. 1. The four-coordinated aluminium center forms a distorted tetrahedral geometry where the bond lengths of Al-N(pyrrole) and Al-N(NH^{t}Bu) are 1.8788(10) and 2.0275(10) Å, respectively. The geometry of **2** is relatively similar to that of the published [C_4H_3N(2-CH_2NMe_2)]$AlMe_2$ complex,[17] indicating the steric congestion of NH^{t}Bu is similar to that of NMe_2.

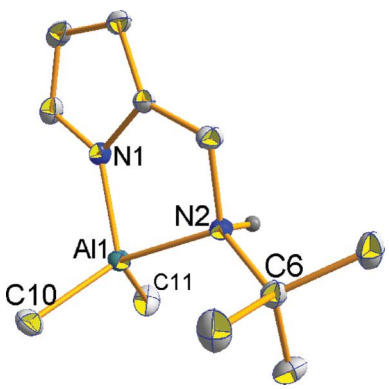

Fig. 1 The molecular structure of complex **1** with the thermal ellipsoids drawn at 30% probability. All hydrogen atoms excepting the amino proton of NH^{t}Bu are omitted for clarity.

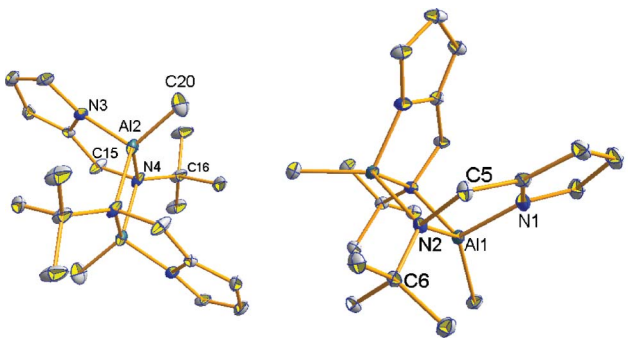

Fig. 2 The molecular structure of complex **2** with the thermal ellipsoids drawn at 30% probability. All hydrogen atoms are omitted for clarity.

Pure yellow-orange crystals of **2** were generated from a toluene solution after repeating recrystallization. Fig. 2 shows a perspective drawing of the molecule **2**, containing two molecular units, together with the selective atomic labelling. The geometries of two independent molecular units in **2** both contain planar Al_2N_2 cores. The pyrrolyl ligands here act as a bidentate dianionic ligand, [C_4H_3N(2-CH_2N^tBu)]$^{2-}$, showing the binding of the pyrrolyl nitrogen terminally to the aluminium atom and the bridging participation of the N^{t}Bu amino nitrogen among two aluminium atoms. The corresponding three rings, AlNCCN, Al_2N_2, and AlCCN are presented in both molecular units of **2**, which are arranged as a chair conformation in the geometry of **2a** and as a boat conformation in the geometry **2b**. Concerning the chair conformation with regard to the Al_2N_2 core, this represents *trans* while *cis* refers to boat form. A schematic drawing showing the geometries of **2** is depicted in Scheme 6. The bond lengths of Al–N(pyrrole) and Al–N(N^{t}Bu) for the geometries of **2a** and **2b** are relatively similar and belong in the range of 1.8365–1.8459 Å and 1.9655–1.9665 Å, respectively. The results are

Table 2 Selected bond lengths (Å) and angles (°) for complexes **1–7** and **9**

1			
Al(1)–N(1)	1.8788(10)	C(11)–Al(1)–C(10)	115.68(7)
Al(1)–C(11)	1.9554(15)	N(1)–Al(1)–N(2)	85.58(4)
Al(1)–C(10)	1.9608(14)	C(11)–Al(1)–N(2)	111.26(6)
Al(1)–N(2)	2.0275(10)	C(10)–Al(1)–N(2)	114.63(5)
N(1)–Al(1)–C(10)	111.78(5)		
2			
Al(1)–N(1)	1.8459(14)	N(1)–Al(1)–N(2A)	109.33(6)
Al(1)–C(10)	1.9550(15)	C(10)–Al(1)–N(2A)	121.54(6)
Al(1)–N(2A)	1.9665(12)	N(1)–Al(1)–N(2)	90.17(5)
Al(1)–N(2)	1.9818(12)	C(10)–Al(1)–N(2)	127.70(6)
Al(1)–Al(1A)	2.7832(8)	N(2A)–Al(1)–N(2)	90.35(5)
Al(2)–N(3)	1.8365(13)	N(3)–Al(2)–C(20)	112.42(15)
Al(2)–C(20)	1.943(2)	N(3)–Al(2)–N(4A)	114.08(6)
Al(2)–N(4A)	1.9655(14)	C(20)–Al(2)–N(4A)	117.85(8)
Al(2)–N(4)	1.9668(13)	N(3)–Al(2)–N(4)	90.01(5)
Al(2)–Al(2A)	2.8073(10)	C(20)–Al(2)–N(4)	129.40(8)
N(1)–Al(1)–C(10)	112.38(7)	N(4A)–Al(2)–N(4)	88.89(5)
3			
Al(1)–N(1)	1.842(2)	N(3)–Al(1)–C(19)	113.04(11)
Al(1)–N(3)	1.855(2)	N(1)–Al(1)–N(2)	86.87(10)
Al(1)–C(19)	1.935(2)	N(3)–Al(1)–N(2)	105.67(9)
Al(1)–N(2)	1.987(2)	C(19)–Al(1)–N(2)	118.47(11)
Al(2)–N(5)	1.850(2)	N(5)–Al(2)–N(7)	113.72(10)
Al(2)–C(38)	1.937(2)	N(1)–Al(1)–N(3)	113.61(10)
Al(2)–N(6)	1.974(2)	N(1)–Al(1)–C(19)	116.35(10)
Al(2)–N(7)	1.854(2)	N(7)–Al(2)–C(38)	112.43(11)
N(5)–Al(2)–N(6)	86.75(10)	N(5)–Al(2)–C(38)	117.48(10)
N(7)–Al(2)–N(6)	104.04(9)	C(38)–Al(2)–N(6)	119.52(12)
4			
Al(1)–O(1)	1.7178(11)	C(11)–O(1)–Al(1)	161.82(10)
Al(1)–N(1)	1.8618(14)	O(1)–Al(1)–N(1)	114.17(6)
Al(1)–C(10)	1.9470(18)	O(1)–Al(1)–N(2)	98.92(6)
Al(1)–N(2)	2.0303(15)	O(1)–Al(1)–C(10)	118.26(7)
C(11)–O(1)	1.3700(17)	N(1)–Al(1)–C(10)	113.81(7)
N(1)–Al(1)–N(2)	85.72(6)	C(10)–Al(1)–N(2)	121.09(7)
5			
Al(1)–N(1)	1.8709(11)	N(1)–Al(1)–C(2)	117.88(6)
Al(1)–C(2)	1.9662(13)	N(1)–Al(1)–C(1)	120.16(5)
Al(1)–C(1)	1.9687(12)	C(2)–Al(1)–C(1)	121.19(6)
Al(1)–N(2)	2.2855(11)	N(1)–Al(1)–N(2)	77.94(4)
Al(1)–N(5)	2.5301(13)	C(2)–Al(1)–N(2)	103.07(5)
6			
Al(1)–N(3)	1.881(2)	N(3)–Al(1)–C(15)	117.53(9)
Al(1)–C(15)	1.970(2)	N(3)–Al(1)–C(18)	114.01(9)
Al(1)–C(18)	1.971(2)	C(15)–Al(1)–C(18)	120.14(10)
Al(1)–N(1)	2.112(2)	N(3)–Al(1)–N(1)	81.96(7)
C(18)–Al(1)–N(1)	109.48(8)	C(15)–Al(1)–N(1)	105.86(8)
7			
Li(1)–N(2)	2.023(3)	N(2)–Li(1)–N(6)	131.29(17)
Al(1)–N(5)	1.7993(14)	N(5)–Al(1)–N(3)	133.72(7)
Li(1)–N(6)	2.030(3)	N(2)–Li(1)–N(1)	92.25(14)
Al(1)–N(3)	1.8083(14)	N(5)–Al(1)–N(4)	90.50(6)
Li(1)–N(1)	2.238(4)	N(6)–Li(1)–N(1)	126.28(16)
Al(1)–N(4)	1.8963(15)	N(3)–Al(1)–N(4)	117.35(7)
Li(1)–N(4)	2.308(3)	Al(1)–N(1)	1.8973(14)
N(2)–Li(1)–N(4)	124.93(16)	N(5)–Al(1)–N(1)	116.73(7)
N(6)–Li(1)–N(4)	90.49(12)	N(3)–Al(1)–N(1)	89.99(6)
Al(1)–N(1)–Li(1)	84.02(9)	N(4)–Al(1)–N(1)	108.54(6)
Al(1)–N(4)–Li(1)	82.13(9)		
9			
Al(1)–O(1)	1.7612(11)	C(21)–O(1)–Al(1)	134.20(9)
Al(1)–N(1)	2.2374(13)	O(1)–Al(1)–N(2)	116.11(6)
Al(1)–N(3)	2.2552(13)	N(1)–Al(1)–N(3)	156.97(5)
Al(1)–N(2)	1.8299(13)	N(2)–Al(1)–N(3)	78.13(5)
C(21)–O(1)	1.3646(17)	N(1)–Al(1)–N(2)	79.03(5)

comparable with the previously published article.[17] It is remarkable to note that **2** consists of two independent geometries (chair form, **2a**; boat form, **2b**), which is not observed in the case of $[\{C_4H_3N(2\text{-}CH_2NMe)\}AlMe]_2$.[17] Comparing the geometries of **1** and $[C_4H_3N(2\text{-}CH_2NMe_2)]AlMe_2$, we have concluded that both the NH^{t}Bu and NMe_2 fragments face similar sterical hindrance. Therefore, the geometries of **2a** and **2b** in the unit cell of **2** may arise accidentally from the crystal packing. Another batch of crystals of complex **2** has been selected and subjected for structural determination. Only the chair form of **2** can be observed in that structure (see ESI†). Obviously, the formation energies of the two conformations of complex **2** (chair and boat form) are relatively similar and this will be discussed *vide infra*.

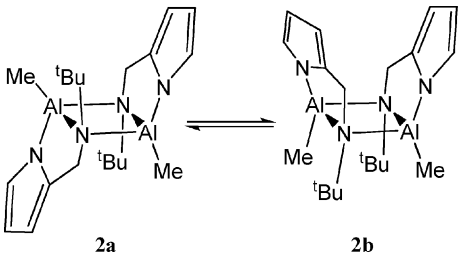

2a **2b**

Scheme 6

Dark red crystals of **3** were obtained from a saturated toluene solution at −20 °C and its molecular structure is shown in Fig. 3. There are two independent molecules in a unit cell; however, these two molecules are very similar. Two equiv. of pyrrolyl ligands $[C_4H_3N(2\text{-}CH_2NH^tBu)]$ coordinate to one aluminium atom. One acts as a bidentate ligand while the other one acts as a monodentate ligand. The aluminium atom is surrounded by three nitrogen atoms and one methyl group forming a distorted tetrahedral geometry. The biting angle of the bidentate pyrrolyl ligand is 86.75(10)°. The two Al–N(pyrrole) bond lengths are relatively close, (1.842(2) Å and 1.855(2) Å) whereas one of the Al–N(NH^{t}Bu) bond lengths belongs in the coordinating range (1.987(2) Å)[18] while the other differentiates far from the bonding range (~3.788 Å).

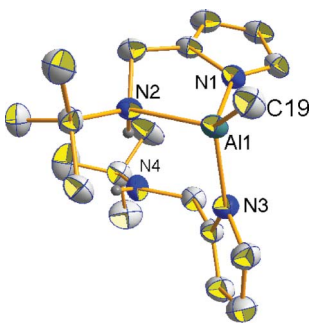

Fig. 3 The molecular structure of complex **3** with the thermal ellipsoids drawn at 30% probability. All hydrogen atoms excepting the amino proton of NH^{t}Bu are omitted for clarity.

Dark red crystals of **4** were obtained from a saturated toluene solution at −20 °C and its molecular structure is shown in Fig. 4. The geometry of **4** is similar to that of **3**. The aluminium center is surrounded by two nitrogen atoms of the bidentate pyrrolyl ligand, methyl group, and aryloxide fragment forming a distorted tetrahedral geometry where the biting angle of the bidentate pyrrolyl ligand is 85.72(6)°. The bond angle of Al(1)–O(1)–C(11) is 161.82(10)° and the bond lengths of Al(1)–O(1) and O(1)–C(11) are 1.7178(11) Å and 1.3700(17) Å, respectively. The short Al–O

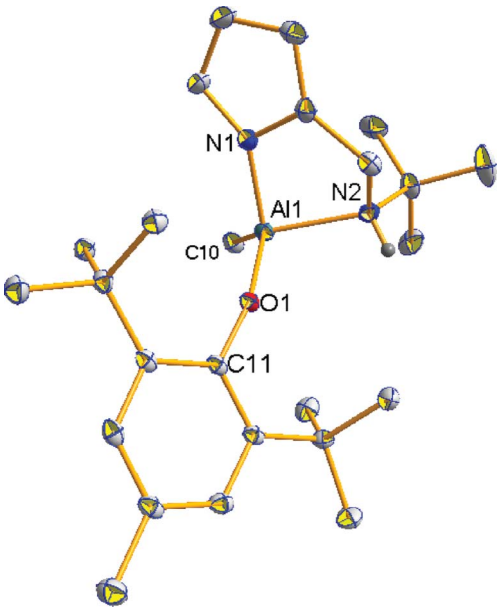

Fig. 4 The molecular structure of complex **4** with the thermal ellipsoids drawn at 30% probability. All hydrogen atoms excepting the amino proton of NH^{t}Bu are omitted for clarity.

bond length and the large Al–O–C bond angle are consistent with the results of Barron's study showing the π-bonding between the aryloxide oxygen and the vacant aluminium p_z orbital.[19]

The molecular structures of **5** and **6** are relatively similar and possess highly distorted geometries, shown in Fig. 5 and 6, respectively, into which the pincer type [C_4H_2(2,5-$CH_2NH^tBu)_2$] acts most likely as a bidentate ligand. The nitrogen atom of the CH_2NH^tBu fragment on the pyrrolyl ring binds the Al atom in an asymmetrical manner. For complex **5**, the Al(1)–N(2) and Al(1)–N(5) bond lengths are 2.2855(11) Å and 2.5301(13) Å, respectively, which correspond to the coordination of one of the two side arms of the pyrrolyl ligand, CH_2NH^tBu, to the Al atom while the other belongs on the borderline of bonding or nonbonding range. Similarly in **6**, the corresponding Al(1)–N(1) and Al(1)–N(2) bond lengths are 2.112(2) Å and 3.018(2) Å, respectively, representing the coordination of one fragment of the pyrrolyl ligand, CH_2NH^tBu, to the Al atom while the other exists as nonbonding to the central tetrahedron unit. However, the solution ^{1}H NMR spectra of **5** and **6** both show only one ^{t}Bu group even at

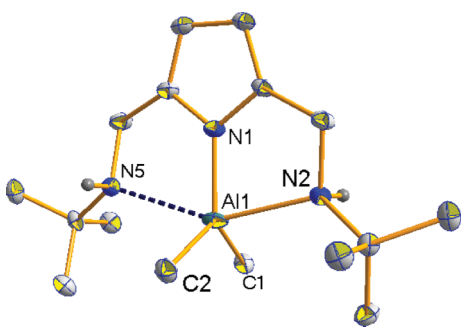

Fig. 5 The molecular structure of complex **5** with the thermal ellipsoids drawn at 50% probability. All hydrogen atoms excepting the amino protons are omitted for clarity.

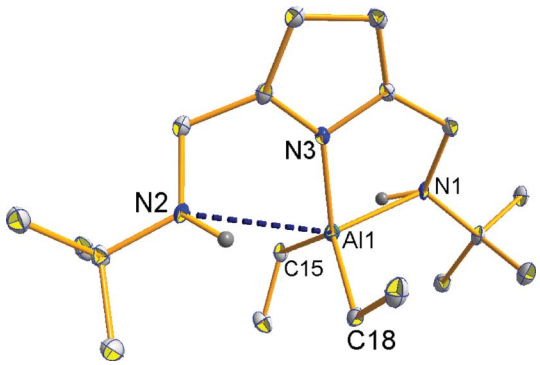

Fig. 6 The molecular structure of complex **6** with the thermal ellipsoids drawn at 50% probability. All hydrogen atoms excepting the amino protons are omitted for clarity.

–60 °C, representing the fast exchange of the bonding of the two NH^{t}Bu fragments to the Al atom.

Pale yellow crystals of **7** were obtained from a toluene solution at –20 °C. The structure of **7** is shown in Fig. 7. Complex **7** is a heterobimetallic complex consisting of two pyrrolyl ligands, one aluminium, and one lithium atom,[20] with one disordered toluene molecule remaining in the lattice. The two pyrrolyl nitrogen atoms bridge to the aluminium and lithium atoms forming an AlN_2Li four-membered ring. The aluminium atom also individually generates a distorted tetrahedron with four nitrogen donor sites, from a pair of pyrrolyl ligands manifesting with pyrrolyl-N and N^{t}Bu fragments of corresponding ligands. The relatively short bond lengths of Al(1)–N(3) and Al(1)–N(5) (*ca.* 1.80 Å) indicating the aluminium with terminal t-butylamido bonding modes is comparable to previous literature.[21] The lithium atom also possesses a distorted tetrahedral environment initiating from four nitrogen donor sites (pyrrolyl-N and NH^{t}Bu fragments) of two corresponding pyrrolyl ligands and the related Li–N(NH^{t}Bu) bond lengths, Li(1)–N(2) and Li(1)–N(6) (av. 2.026 Å) belong in the normal range, like in other published articles.[22]

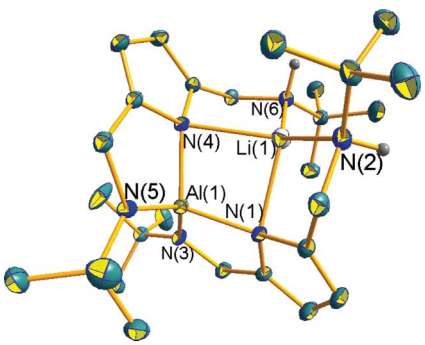

Fig. 7 The molecular structure of complex **7** with the thermal ellipsoids drawn at 50% probability. All hydrogen atoms excepting the amino protons are omitted for clarity.

Orange crystals of **9** were obtained from a diethyl ether solution at –20 °C and its molecular structure was shown in Fig. 8. The geometry of **9** can be emphasized as a distorted trigonal bipyramidal. The tridentate pyrrolyl ligand is connected to aluminium atom in a symmetrical *mer*-type where the pyrrolyl ring nitrogen occupies the equatorial position and two NH^{t}Bu

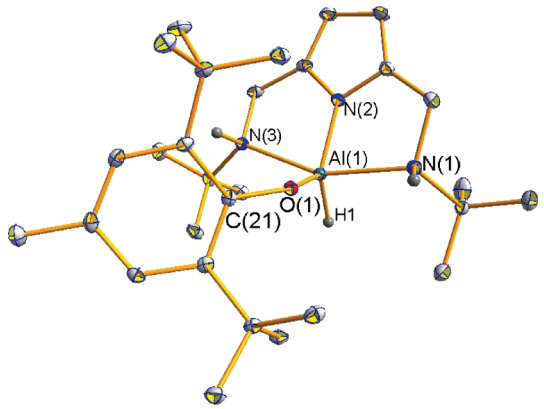

Fig. 8 The molecular structure of complex **9** with the thermal ellipsoids drawn at 50% probability. All hydrogen atoms excepting the hydride and amino protons are omitted for clarity.

nitrogen atoms feature the axial sites with the bond angle of N(3)–Al(1)–N(1) at 156.97(5)°. The trigonal plane has been formed by the pyrrolyl ring nitrogen, hydride and the oxygen atom of aryloixde fragment. In contrast to complex **4**, the relative small bond angle of Al(1)–O(1)–C(21) (134.20(9)°) representing less interactions of the π-bonding between the aryloxide oxygen and the vacant aluminium p_z orbital.

Dynamic properties of complex 2

The geometries of complexes containing one Al_2N_2 core and two rings formed by the coordination of bidentate dianionic ligands to the aluminium atom exist in two possible conformations, chair-form and boat-form. Most of the complexes in the systems A-E in Scheme 7 have chair-form geometries due to the steric congestion.[13a,23] However, we have found that for system E in Scheme 6 there exists one complex with a boat-form conformation.[24] In the case of complex **2** of this paper, two geometries (boat- and chair-form) are observed. Theoretical computations using the B3LYP density functional and the 6-31G(d) basis set revealed that the enthalpy of the chair-form (**2a**) at 298 K is 2.63 kcal mol^{-1} lower than that of the boat-form (**2b**). The results suggest that in the presence of the bulky t-butyl group plays an important role on its conformation and that thermodynamically the chair- and boat-forms can be converted (Scheme 7). The variable temperature ^{1}H NMR spectra of **2** (Fig. 9, from 353 K to 188 K) also proves this phenomenon. At high temperature (353 K), only one set of methyl, t-butyl, methylene, and pyrrolyl protons were observed. While the solution temperature was lowered to 188 K, the t-butyl and pyrrolyl groups both split into two resonances and the others remain unchanged. A reasonable explanation for the dynamic properties of **2** is that

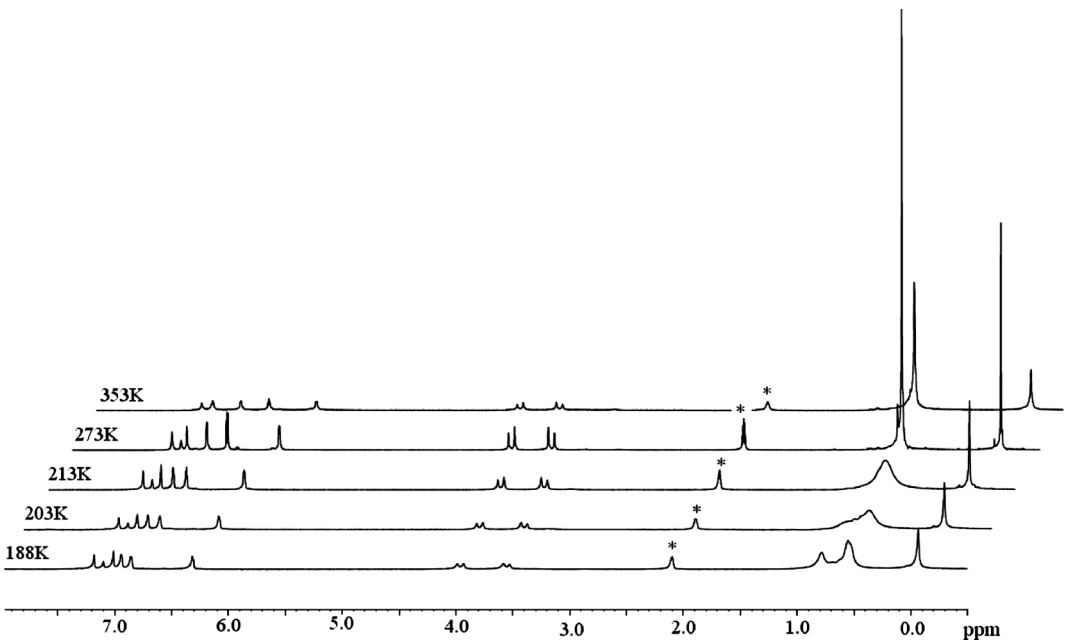

Fig. 9 The variable temperature ^{1}H NMR spectra of complex **2** in d^8-toluene using 300 MHZ NMR spectrometer. The solvent peak was designated as a start mark.

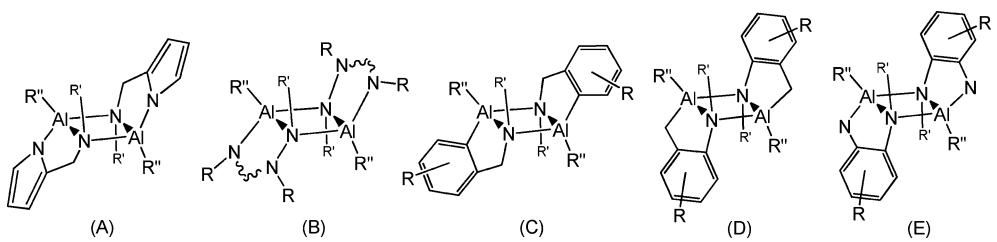

Scheme 7

Table 3 Polymerization of ε–caprolactone (CPL) using complex **4** as an initiator

entry	$[CPL]_0/[4]_0$	conversion (%)	activity[a]	$M_{n,theor}$[b]	$M_{n,cor}$[c]	PDI	f (%)[d]
1	50	99	5500	5650	39700	1.68	14
2	100	99	11140	11300	51900	1.42	21
3	150	99	16340	16950	126000	1.21	13
4	300	98	33280	33557	166700	1.09	20

[a] $g_{pol}mol_{cat}^{-1}\cdot h^{-1}$; [b] $M_{n,theor} = ([CPL]_0/[4]_0) \times 114.14 \times$ conversion (%) for CPL; [c] $M_{n,cor} = 0.259\ M_{n,GPC,St}^{1.073}$ for CPL[e]; [d] initiator efficiency = $M_{n,theor}/M_{n,cor}$; [e] P. Dubois, I. Barakat, R. Jerome, P. Teyssie *Macromolecules*, **1993**, *26*, 4407. rxn temp/time(m) = 75 °C

the low differentiate of formation enthalpy of chair-form **2** (**2a**) and boat-form **2** (**2b**) results in the fast exchange between the two conformations. In addition, the spectrum at 188 K only slightly slows the exchange rate and most of the dynamic properties of **2** remain unchanged.

Ring opening polymerization of ε-caprolactone catalyzed by 4

Aluminium phenoxide **4** can be treated as an initiator for the ring opening polymerization of ε-caprolactone, and the corresponding results are presented in Table 3. There was an increase in molecular weight (M_n) and decrease in molecular weight distribution (PDI) on increasing the feeding ratio of the monomer to the catalyst ($[CPL]_0/[4]_0$). However, poor linear correlation between M_n and $[CPL]_0/[4]_0$ was observed, which could result from slow initiation rate. The observed M_n's significant deviations from the theoretical molecular weights also indicates that the initiation would be slow in comparison with propagation, and the initiation might have not been quantitative. The polymerization activity of **4** is comparable to that of previously reported neutral and cationic aluminium complexes[25] supported by bidentate *O*,*P*-phosphinophenolate ligands, neutral aluminium heteroscorpionate,[26] diamides[27] or ketiminate[13c] complexes. Comparing the increase in molecular weight (M_n) while applying different entries, there is a decrease in the PDI values for aluminium phenoxide with the treatment of ε-caprolactone whereas the numerical molecular weights obtained for the polymers increase with the [M]/[Al] ratio in the feed of polymerization runs. These are subsequently higher than theoretical ones ($M_{n,theor}$) for heteroscorpionate aluminium complexes[26] and subject to the $M_{n,theor}$ value remaining constant, the PDI values varied with the $M_{n,obs}$ values for *O*,*P*-phosphinophenolate mediated aluminium derivatives.[25]

Conclusions

In summary, the reactivities of $[C_4H_3NH(2\text{-}CH_2NH^tBu)]$ and $[C_4H_2NH(2,5\text{-}CH_2NH^tBu)_2]$ with AlR_3 and $LiAlH_4$ under different conditions were investigated and characterized mainly by NMR spectroscopic data analyses. Using the aluminium alkoxide derivative $[C_4H_3N(2\text{-}CH_2NH^tBu)][OC_6H_2(\text{-}2,6\text{-}^tBu_2\text{-}4\text{-}Me)]AlMe$ (**4**) as an initiator, moderate reactivity towards ring opening polymerization of ε-caprolactone was observed . We have isolated one novel complex, $[C_4H_2N(2\text{-}CH_2N^tBu)(5\text{-}CH_2NH^tBu)]_2AlLi$ (**7**), after repeating re-crystallization for the reaction between $LiAlH_4$ and one equiv. of $C_4H_2NH(2,5\text{-}CH_2NH^tBu)_2$ in diethyl ether at 0 °C, where we subsequently observed the evolution of hydrogen gas. Future work will explore the design of synthesizing asymmetric pyrrolyl ligands and study the reactivity for main group metal chemistry and inserting lanthanides, as well as different organic molecules. It will be our priority to differentiate metal–ligand based architecture over hydroalumination and insertion reactions.

Experimental

Physical measurements and materials

All reactions were performed under a dry nitrogen atmosphere using standard Schlenk techniques or in a glove box. Toluene and diethyl ether were dried by refluxing over sodium benzophenone ketyl. CH_2Cl_2 was dried over P_2O_5. All solvents were distilled and stored in solvent reservoirs, which contained 4 Å molecular sieves and were purged with nitrogen. ^1H and ^{13}C NMR spectra were recorded on a Bruker Avance 300 spectrometer. Chemical shifts for ^1H and ^{13}C spectra were recorded in ppm relative to the residual protons of $CDCl_3$ (δ 7.24, 77.0) and C_6D_6 (δ 7.15, 128.0). Elemental analyses were performed on a Heraeus CHN-OS Rapid Elemental Analyzer at the Instrument Center of the NCHU. Due to higher air sensitivity, we could not collect elemental analysis data for compounds **2**, **3**, **5** and **7**. $[C_4H_3NH(2\text{-}CH_2NH^tBu)]$ and $[C_4H_2NH(2,5\text{-}CH_2NH^tBu)_2]$ were prepared in a similar procedure as reported in the literature.[13a] All the chemicals (Aldrich, Acros) were used as received.

Preparation of the complexes

Synthesis of $[C_4H_3N(2\text{-}CH_2NH^tBu)]AlMe_2$ (1). To a solution of $AlMe_3$ (3.16 mL, 3.28 mmol) in 10 mL of toluene was added dropwise a $C_4H_3NH(2\text{-}CH_2NH^tBu)$ (0.50 g, 3.28 mmol) toluene solution (20 mL) at 25 °C. The mixture was stirred at room temperature for 12 h and the color changed from colorless to pale orange yellow. Volatiles were removed under vacuum and the solid was re-crystallized from a toluene solution at –20 °C to yield 0.51 g (74%) of orange-red solid. ^1H NMR (C_6D_6): –0.28 (s, 6H, AlMe_2), 0.65 (s, 9H, NHCMe_3), 2.13 (s, 1H, CH_2NHCMe_3), 3.40 (dd, 2H, CH_2NH), 6.23 (d, 1H, pyrrolyl C*H*), 6.63 (t, 1H, pyrrolyl C*H*), 7.01 (s, 1H, pyrrolyl C*H*). ^{13}C NMR (C_6D_6): –7.77 (AlMe_2), 27.2 (q, J_{CH} = 126 Hz, NHCMe_3), 42.4 (t, J_{CH} = 141 Hz, CH_2NHCMe$_3$), 54.1 (s, NCMe_3), 103.5 (d, J_{CH} = 164 Hz, pyrrolyl *C*H), 111.1 (d, J_{CH} = 165 Hz, pyrrolyl *C*H), 122.1 (d, J_{CH} = 178 Hz, pyrrolyl *C*H), 132.2 (s, pyrrolyl C_{ipso}). Anal. calcd for $C_{11}H_{21}AlN_2$ (208.28): C 63.43, H 10.16, N 13.45. Found: C 62.44, H 9.95, N 13.68%.

Synthesis of $[\{C_4H_3N(2\text{-}CH_2N^tBu)\}AlMe]_2$ (2). Similar procedures as for synthesizing complex **1** were used except the addition was performed at 0 °C and then heated at 93 °C for 24 h. Repeating

re-crystallizations were carried out due to the mixture of complexes **1** and **2**. 0.39 g of yellow-orange crystals were obtained (31% yield). ^{1}H NMR (C_6D_6): –0.17 (s, 6H, Al*Me*), 0.75 (s, 18H, NHC*Me*$_3$), 3.83 4.21 (dd, $^2J_{HH}$ = 16.2 Hz, 4H, *CH*$_2$NHCMe$_3$), 6.20 (d, 2H, pyrrolyl C*H*), 6.67 (t, 2H, pyrrolyl C*H*), 6.85 (d, 2H, pyrrolyl C*H*). ^{13}C NMR (C_6D_6): 28.8 (q, J_{CH} = 126 Hz, NC*Me*$_3$), 45.3 (t, J_{CH} = 138 Hz, *C*H$_2$NCMe$_3$), 56.4 (s, N*C*Me$_3$), 104.2 (d, J_{CH} = 165 Hz, pyrrolyl *C*H), 114.6 (d, J_{CH} = 161 Hz, pyrrolyl *C*H), 120.9 (d, J_{CH} = 180 Hz, pyrrolyl *C*H), 137.4 (s, pyrrolyl *C*$_{ipso}$).

Synthesis of [C$_4$H$_3$N(2-CH$_2$NH^{t}Bu)]$_2$AlMe (3). Similar procedures as for synthesizing complex **1** were adopted. C$_4$H$_3$NH(2-CH$_2$NH^{t}Bu) (1.00 g, 6.56 mmol) and AlMe$_3$ (3.16 mL, 3.28 mmol) were used and the reaction was stirred at room temperature for 12 h. Dark red crystals were obtained from a toluene solution to afford 0.42 g of **3** in 37% yield. ^{1}H NMR (C_6D_6): –0.17 (s, 3H, Al*Me*), 0.82 (s, 18H, NHC*Me*$_3$), 3.44 (dd, 4H, *CH*$_2$NH), 3.83 (s, 2H, CH$_2$N*H*CMe$_3$), 6.18 (d, 2H, pyrrolyl C*H*), 6.46 (t, 2H, pyrrolyl C*H*), 6.89 (s, 2H, pyrrolyl C*H*). ^{13}C NMR (C_6D_6): 28.1 (q, J_{CH} = 126 Hz, NHC*Me*$_3$), 41.4 (t, J_{CH} = 137 Hz, *C*H$_2$NHCMe$_3$), 52.4 (s, N*C*Me$_3$), 108 (d, J_{CH} = 165 Hz, pyrrolyl *C*H), 111.4 (d, J_{CH} = 165 Hz, pyrrolyl *C*H), 124.4 (d, J_{CH} = 179 Hz, pyrrolyl *C*H), 134.8 (s, pyrrolyl *C*$_{ipso}$).

Synthesis of [C$_4$H$_3$N(2-CH$_2$NH^{t}Bu)][OC$_6$H$_2$(-2,6-^{t}Bu$_2$-4-Me)]AlMe (4). To a solution of **1** (0.20 g, 0.96 mmol) in 10 mL of toluene was added dropwise a HOC$_6$H$_2$(-2,6-^{t}Bu$_2$-4-Me) (0.21 g, 0.96 mmol) toluene solution (20 mL) at 0 °C. The mixture was stirred at room temperature for 4 h and the color changed from colorless to dark red. Volatiles were removed under vacuum and the solid was re-crystallized from a toluene solution to yield 0.18 g (45%) of dark red solid. ^{1}H NMR (C_6D_6): –0.09 (s, 3H, Al*Me*), 0.8 (s, 9H, NHC*Me*$_3$), 1.46 (s, 18H, C*Me*$_3$), 2.33 (s, 3H, *Me*), 3.27 (s, 1H, CH$_2$N*H*CMe$_3$), 3.46 (d, $^2J_{HH}$ = 15 Hz, 1H, *CH*$_a$H$_b$NH), 4.08 (d, $^2J_{HH}$ = 9 Hz, 1H, *CH*$_a$*H*$_b$NH), 6.2 (d, 1H, pyrrolyl C*H*), 6.62 (t, 1H, pyrrolyl C*H*), 7.11 (s, 1H, pyrrolyl C*H*), 7.21 (s, 2H, phenyl C*H*). ^{13}C NMR (C_6D_6): –7.0 (br, Al*Me*), 21.4 (q, J_{CH} = 125 Hz, *Me*), 27.8 (q, J_{CH} = 127 Hz, NHC*Me*$_3$), 31.2 (q, J_{CH} = 128 Hz, C*Me*$_3$), 34.7(s, *C*Me$_3$), 42.9 (t, J_{CH} = 140 Hz, *C*H$_2$NHCMe$_3$), 56.4 (s, N*C*Me$_3$), 103.9 (d, J_{CH} = 160 Hz, pyrrolyl *C*H), 111.7 (d, J_{CH} = 166 Hz, pyrrolyl *C*H), 123.4 (d, J_{CH} = 180 Hz, pyrrolyl *C*H), 125.8 (s, phenyl C*H*), 126.5 (s, phenyl *C*$_{ipso}$), 133.4 (s, pyrrolyl *C*$_{ipso}$), 138.3 (s, phenyl *C*$_{ipso}$), 154.2 (s, phenyl *C*$_{ipso}$). Anal. calcd for C$_{25}$H$_{41}$AlN$_2$O (412.59): C 72.78, H 10.02, N 6.79. Found: C 71.83, H 10.92, N 6.55%.

Synthesis of [C$_4$H$_2$N(2,5-CH$_2$NH^{t}Bu)$_2$]AlMe$_2$ (5). To a solution of AlMe$_3$ (1.05 mL, 2.10 mmol) in 10 mL of toluene was added dropwise a C$_4$H$_2$NH(2,5-CH$_2$NH^{t}Bu)$_2$ (0.50 g, 2.10 mmol) toluene solution (20 mL) at 0 °C. The mixture was stirred at room temperature for 12 h and then volatiles were removed under vacuum. The solid was re-crystallized from a diethyl ether solution to yield 0.41 g (67%) of yellow-orange solid. ^{1}H NMR (C_6D_6): –0.31 (s, 6H, Al*Me*$_2$), 0.94 (s, 18H, NHC*Me*$_3$), 1.59 (s, 2H, CH$_2$N*H*CMe$_3$), 3.62 (dd, $^2J_{HH}$ = 8.4 Hz, 1H, C*H*$_a$H$_b$NH), 3.65 (dd, $^2J_{HH}$ = 8.4 Hz, 1H, CH$_a$*H*$_b$NH), 6.38 (s, 2H, pyrrolyl C*H*). ^{13}C NMR (C_6D_6): –4.9 (s, Al*Me*$_2$), 25.6 (q, J_{CH} = 125 Hz, NHC*Me*$_3$), 42 (t, J_{CH} = 128 Hz, *C*H$_2$NHCMe$_3$), 52.5 (s, N*C*Me$_3$), 104.7 (d, J_{CH} = 164 Hz, pyrrolyl *C*H), 132.6 (s, pyrrolyl *C*$_{ipso}$).

Synthesis of [C$_4$H$_2$N(2,5-CH$_2$NH^{t}Bu)$_2$]AlEt$_2$ (6). To a solution of AlEt$_3$ (1.05 mL, 2.10 mmol) in 10 mL of toluene was added dropwise a C$_4$H$_2$NH(2,5-CH$_2$NH^{t}Bu)$_2$ (0.50 g, 2.10 mmol) toluene solution (20 mL) at 0 °C. The mixture was stirred at room temperature for 12 h and then volatiles were removed under vacuum. The solid was re-crystallized from a toluene solution to yield 0.42 g (62%) of pale yellow-orange solid. ^{1}H NMR (C_6D_6): 0.31 (q, 4H, AlC*H*$_2$CH$_3$), 0.93 (s, 18H, NHC*Me*$_3$), 1.26 (t, 6H, AlCH$_2$C*H*$_3$), 1.63 (s, 2H, CH$_2$N*H*CMe$_3$), 3.67 (dd, $^2J_{HH}$ = 9 Hz, 1H, C*H*$_a$H$_b$NH), 3.70 (dd, $^2J_{HH}$ = 9 Hz, 1H, CH$_a$*H*$_b$NH), 6.34 (s, 1H, pyrrolyl C*H*). ^{13}C NMR (C_6D_6): 2.6 (t, J_{CH} = 112 Hz, Al*C*H$_2$CH$_3$), 9.8 (q, J_{CH} = 118 Hz, AlCH$_2$*C*H$_3$), 28.5 (q, J_{CH} = 125 Hz, NHC*Me*$_3$), 42.5 (t, J_{CH} = 136 Hz, *C*H$_2$NHCMe$_3$), 52.4 (s, N*C*Me$_3$), 105.2 (d, J_{CH} = 165 Hz, pyrrolyl *C*H), 133.4 (s, pyrrolyl *C*$_{ipso}$). Anal. calcd for C$_{18}$H$_{36}$AlN$_3$ (321.48): C 67.25, H 11.29, N 13.07. Found: C 67.29, H 10.73, N 13.63%.

Synthesis of [C$_4$H$_2$N(2-CH$_2$N^{t}Bu)(5-CH$_2$NH^{t}Bu)]$_2$AlLi (7). To a solution of LiAlH$_4$ (0.080 g, 2.10 mmol) in 10 mL of toluene was added dropwise a C$_4$H$_2$NH(2,5-CH$_2$NH^{t}Bu)$_2$ (0.50 g, 2.10 mmol) toluene solution (20 mL) at 0 °C. The mixture was stirred at room temperature for 12 h and then volatiles were removed under vacuum. The solid was re-crystallized from a toluene solution to yield 0.223 g (21%) of pale yellow solid. ^{1}H NMR (C_6D_6): 0.59 (s, 18H, NHC*Me*$_3$), 1.31 (s, 18H, NC*Me*$_3$), 3.51 (dd, 2H, C*H*$_a$H$_b$NH), 3.90 (dd, 2H, CH$_a$*H*$_b$NH), 4.36 (q, 4H, C*H*$_2$NCMe$_3$), 6.29 (s, 2H, pyrrolyl C*H*), 6.41 (s, 2H, pyrrolyl C*H*). ^{13}C NMR (C_6D_6): 8.3 (q, J_{CH} = 128 Hz, NC*Me*$_3$), 30.4 (q, J_{CH} = 124 Hz, NHC*Me*$_3$), 41.1 (t, J_{CH} = 136 Hz, *C*H$_2$NHCMe$_3$), 44.0 (t, J_{CH} = 133 Hz, *C*H$_2$NCMe$_3$), 50.5 (s, NH*C*Me$_3$), 50.8 (s, N*C*Me$_3$), 104.3 (d, J_{CH} = 167 Hz, pyrrolyl *C*H), 112.4 (d, J_{CH} = 163 Hz, pyrrolyl *C*H), 129.3 (s, pyrrolyl *C*$_{ipso}$), 130.3 (s, pyrrolyl *C*$_{ipso}$), 145.9 (s, toluene C$_{ipso}$).

Synthesis of [C$_4$H$_2$N(2,5-CH$_2$NH^{t}Bu)$_2$]AlH$_2$ (8). To a solution of Me$_3$N·HCl (2.00 g, 2.090 mmol) in 20 mL of diethyl ether was added dropwise a LiAlH$_4$ (0.95 g, 25.1 mmol) diethyl ether solution (20 mL) at 0 °C. The mixture was stirred at room temperature for 2 h and the solution was filtered through Celite. To the filtrate, a diethyl ether (20 mL) solution of C$_4$H$_2$NH(2,5-CH$_2$NH^{t}Bu)$_2$ (4.96 g, 20.9 mmol) was added slowly at 0 °C. The solution was then stirred at room temperature for 12 h. Volatiles were removed to yield a white solid. The solid was re-crystallized from a methylene chloride solution to yield 5.546 g (70%) of colorless solid. ^{1}H NMR (C_6D_6): 1.31 (s, 18H, NHC*Me*$_3$), 2.58 (s, 2H, CH$_2$N*H*CMe$_3$), 3.72 (d, 4H, C*H*$_2$NH), 5.83 (s, 2H, pyrrolyl C*H*). ^{13}C NMR (C_6D_6): 28.4 (q, J_{CH} = 125 Hz, NC*Me*$_3$), 41.9 (t, J_{CH} = 134 Hz, *C*H$_2$NHCMe$_3$), 54.7 (s, N*C*Me$_3$), 104.2 (d, J_{CH} = 168 Hz, pyrrolyl *C*H), 132.3 (s, pyrrolyl *C*$_{ipso}$). Anal. calcd for C$_{14}$H$_{28}$AlN$_3$ (265.379): C 63.36, H 10.63, N 15.83. Found: C 63.29, H 10.76, N 15.81%. IR (KBr): 1801 cm^{-1} ($\nu_{Al\text{-}H}$), 3201 cm^{-1} (ν_{NH}), 1318 cm^{-1} ($\nu_{Al\text{-}D}$)

Synthesis of [C$_4$H$_2$N(2,5-CH$_2$NH^{t}Bu)$_2$]AlH[OC$_6$H$_2$(-2,6-^{t}Bu$_2$-4-Me)] (9). To a solution of **8** (0.20 g, 0.75 mmol) in 10 mL of methylene chloride was added dropwise a HOC$_6$H$_2$(-2,6-^{t}Bu$_2$-4-Me) (0.17 g, 0.75 mmol) methylene chloride solution (20 mL) at 0 °C. The mixture was stirred at room temperature for 2 h and the color changed from colorless to orange. Volatiles were removed under vacuum and the solid was re-crystallized from a diethyl ether solution to yield 0.24 g (67%) of orange solid. ^{1}H NMR (C_6D_6): 0.97 (s, 18H, NHC*Me*$_3$), 1.48 (s, 18H, C*Me*$_3$), 2.28 (s, 3H, phenyl

Me), 2.32 (s, 2H, CH_2NHCMe_3), 3.66–3.80 (m, 4H, CH_2NH), 6.28 (s, 2H, pyrrolyl C*H*), 7.10 (s, 2H, phenyl C*H*). ^{13}C NMR (C_6D_6): 21.1 (q, J_{CH} = 125 Hz, -*Me*), 28.1 (q, J_{CH} = 126 Hz, NHC*Me*$_3$), 32.3 (q, J_{CH} = 125 Hz, o-PhC*Me*$_3$), 35.7 (s, o-Ph*C*Me$_3$), 42.2 (t, J_{CH} = 137 Hz, CH_2NHCMe_3), 54.2 (s, N*C*Me$_3$), 104.8 (d, J_{CH} = 164 Hz, pyrrolyl *C*H), 125.3 (s, phenyl *C*H), 126.6 (s, phenyl C_{ipso}), 131.8 (s, pyrrolyl C_{ipso}), 139.2 (s, phenyl C_{ipso}), 156.5 (s, phenyl C_{ipso}). Anal. calcd for $C_{29}H_{50}AlN_3O$ (483.71): C 72.01, H 10.42, N 8.69. Found: C 71.56, H 9.65, N 8.78%. IR (KBr): 1852 cm^{-1} ($\nu_{Al\text{-}H}$), 3214 cm^{-1} (ν_{NH}), 1342 cm^{-1} ($\nu_{Al\text{-}D}$).

X-Ray crystallography

All the crystals were mounted on a glass fiber using epoxy resin and transferred to a goniostat. Data were collected on a Bruker AXS SMART CCD diffractometer with graphite-monochromated Mo-Kα radiation. Due to the air-sensitivity of these crystals, complexes **1–7** and **9** were covered with oil and transferred to the N_2 stream of the diffractometer during data collection. Intensity data were collected with a combination of ω and ϕ scans. All data were corrected for Lorentz and polarization effects, and the program SADABS in APEX2[28] was used for the absorption correction. The structures were solved by direct and difference Fourier methods. All non-hydrogen atoms were refined with anisotropic displacement parameters. Crystallographic computing was performed using SHELXTL[28] package of programs. All refinements were carried out by full-matrix least squares using anisotropic displacement parameters for all non-hydrogen atoms. All the relevant crystallographic data and structure refinement parameters for **1–7** and **9** are summarized in Table 1.

Crystallographic data for the structures reported in this paper have been deposited with the Cambridge Crystallographic Data Centre with CCDC numbers 792978 (**1**), 792979 (**2**), 792981 (**2**-another set of data), 792982 (**3**), 792980 (**4**), 808790 (**5**), 808793 (**6**), 808792 (**7**) and 808791 (**9**).

Polymerization

Polymerizations were carried out in toluene under a nitrogen-filled Schlenk line. Considering a typical method, the initiator was first dissolved in 5 mL of toluene, followed by the addition of ε-caprolactone, and then stirred at the selected temperature for a period of time to produce a gel- or solid-like polymer. The process continued until the mixture gradually quenched with acidified water (3% CH_3COOH) and the resulting solid was washed with hexane. It was dried to form a satisfactory yield. The molecular weight of the polymers was determined on a gel permeation chromatography (GPC) instrument (Waters, RI 2414, pump 1515). M_n and M_w values were determined from calibration plots established with polystyrene standards.

Theoretical calculation

We used the gradient-corrected hybrid density functional theory (DFT), B3LYP. The approach is a hybrid method, which consists of the three-parameter mixing of Hartree–Fock exchange, gradient-corrected exchange functional of Becke[29] and correlation functional of Lee, Yang, and Parr.[30] All calculations were carried out using the Gaussian 03 program.[31]

Acknowledgements

We acknowledge the financial assistance to the National Science Council of Taiwan. We would wish to thank the National Changhua University of Education for supporting the X-ray diffractometer and NMR spectrometer.

References

1 (*a*) W. Ziemkowska, *Coord. Chem. Rev.*, 2005, **249**, 2176; (*b*) W. Uhl, *Coord. Chem. Rev.*, 2008, **252**, 1540; (*c*) J. Lewinski, J. Zachara, I. Justyniak and M. Dranka, *Coord. Chem. Rev.*, 2005, **249**, 1185; (*d*) H. Yamamoto, Ed., *Lewis Acids in Organic Synthesis, Vol 1*, Wiley-VCH 2000.
2 (*a*) S. Aldridge and A. J. Downs, *Chem. Rev.*, 2001, **101**, 3305; (*b*) L. George and S. K. Saxena, *Int. J. Hydrogen Energy*, 2010, **35**, 5454; (*c*) R. J. Wehmschulte and P. P. Power, *Polyhedron*, 2000, **19**, 1649.
3 (*a*) M. Bochmann, *Acc. Chem. Res.*, 2010, **43**, 1267; (*b*) S. Dagorne and D. A. Atwood, *Chem. Rev.*, 2008, **108**, 4037; (*c*) A. V. Korolev, E. Ihara, I. A. Guzei, V. G. Young, Jr. and R. F. Jordan, *J. Am. Chem. Soc.*, 2001, **123**, 8291.
4 (*a*) O. Dechy-Cabaret, B. Martin-Vaca and D. Bourissou, *Chem. Rev.*, 2004, **104**, 6147; (*b*) M. H. Chisholm, *Inorg. Chim. Acta*, 2009, **362**, 4284; (*c*) S. Dagorne, F. Le Bideau, R. Welter, S. Bellemin-Laponnaz and A. Maisse-Francois, *Chem.–Eur. J.*, 2007, **13**, 3202; (*d*) O. Coulembier, P. Dege'e, J. L. Hedrick and P. Dubois, *Prog. Polym. Sci.*, 2006, **31**, 723.
5 (*a*) H. Sinn, W. Kaminsky, H.-J. Vollmer and R. Woldt, *Angew. Chem., Int. Ed. Engl.*, 1980, **19**, 390; (*b*) H. Sinn and W. Kaminsky, *Adv. Organomet. Chem.*, **18**, 99; (*c*) E. Y.-X. Chen and T. J. Marks, *Chem. Rev.*, 2000, **100**, 1391; (*d*) A. Arbaoui and C. Redshaw, *Polym. Chem.*, 2010, **1**, 801.
6 (*a*) H. C. Brown, P. V. *Ramachandran, ACS Symposium Series*, **1996**, 641, *Reductions in Organic Synthesis, Chapter 1*; (*b*) T. Ikariya and J. Blacker, *Acc. Chem. Res.*, 2007, **40**, 1300.
7 (*a*) F. Schuth, B. Bogdanovic and M. Felderhoff, *Chem. Commun.*, 2004, 2259; (*b*) S. –I. Orimo, Y. Nakamori, J. R. Eliseo, A. Zuttel and C. M. Jensen, *Chem. Rev.*, 2007, **107**, 4111; (*c*) G. Guillena, D. J. Ramón and M. Yus, *Chem. Rev.*, 2010, **110**, 1611.
8 (*a*) R. A. Jones and G. P. Bean, *The Chemistry of Pyrroles*, Academic Press, London, 1977, p 2; (*b*) *Pyrroles. The Synthesis, Reactivity, and Physical Properties of Substituted Pyrroles*, R. A. Jones, Ed., Wiley, New York, 1992; (*c*) R. N. Brogden, R. C. Heel, T. M. Speight and G. S. Avery, *Drugs*, 1978, **15**, 429.
9 R. A. Jones, *Comprehensive Heterocyclic Chemistry*, A. R. Katritsky and C. W. Rees, ed., Pergamon Press, Oxford, 1984, Vol. 4, p 201.
10 (*a*) Z. Yu, J. M. Wittbrodt, A. Xia, M. J. Heeg, H. B. Schlegel and C. H. Winter, *Organometallics*, 2001, **20**, 4301; (*b*) P. T. Lansbury, J. R. Rogozinski and F. L. Coblentz, *J. Org. Chem.*, 1961, **26**, 2277.
11 C.-Y. Lin, C.-F. Tsai, H.-J. Chen, C.-H. Hung, R.-C. Yu, P.-C. Kuo, H. M. Lee and J.-H. Huang, *Chem.–Eur. J.*, 2006, **12**, 3067.
12 (*a*) P.-C. Kuo, I.-C. Chen, J.-C. Chang, M.-T. Lee, C.-H. Hu, C.-H. Hung, H. M. Lee and J.-H. Huang, *Eur. J. Inorg. Chem.*, 2004, 4898; (*b*) J.-C. Chang, C.-H. Hung and J.-H. Huang, *Organometallics*, 2001, **20**, 4445; (*c*) C.-Y. Lin, H. M. Lee and J.-H. Huang, *J. Organomet. Chem.*, 2007, **692**, 3718.
13 (*a*) Y.-C. Chen, C.-Y. Lin, C.-Y. Li, J.-H. Huang, L.-C. Chang and T. –Y. Lee, *Chem.–Eur. J.*, 2008, **14**, 9747; (*b*) W.-Y. Lee, H.-H. Hsieh, C.-C. Hsieh, H. M. Lee, G.-H. Lee, J.-H. Huang, T.-C. Wu and S.-H. Chuang, *J. Organomet. Chem.*, 2007, **692**, 1131; (*c*) R.-C. Yu, C.-H. Hung, J.-H. Huang, H.-Y. Lee and J.-T. Chen, *Inorg. Chem.*, 2002, **41**, 6450.
14 Similar phenomena have been seen, for example: M. P. Coles, D. C. Swenson and R. F. Jordan, *Organometallics*, 1997, **16**, 5183.
15 (*a*) M. E. Van Der Boom and D. Milstein, *Chem. Rev.*, 2003, **103**, 1759; (*b*) C. M. Jensen, *Chem. Commun.*, **1999**, 2443; (*c*) A. Vigalok and D. Milstein, *Acc. Chem. Res.*, 2001, **34**, 798.
16 Y.-L. Lien, Y.-C. Chang, N.-T. Chuang, A. Datta, S.-J. Chen, C.-H. Hu, W.-Y. Huang, C.-H. Lin and J.-H. Huang, *Inorg. Chem.*, 2010, **49**, 136.
17 J.-H. Huang, H.-J. Chen, J.-C. Chang, C.-C. Zhou, G.-H. Lee and S.-M. Peng, *Organometallics*, 2001, **20**, 2647.

18 (*a*) A. Willner, A. Hepp and N. W. Mitzel, *Dalton Trans.*, 2008, 6832; (*b*) M. G. Gardiner, S. M. Lawrence and C. L. Raston, *Inorg. Chem.*, 1995, **34**, 4652.

19 (*a*) M. D. Healy, J. W. Ziller and A. R. Barron, *J. Am. Chem. Soc.*, 1990, **112**, 2949; (*b*) A. R. Barron, *Polyhedron*, 1995, **14**, 3197.

20 Al-Li heterobimetallic compounds, for examples: (*a*) F. Voigt, A. Fischer, C. Pietzsch and K. Jacob, *Z. Anorg. Allg. Chem.*, 2001, **627**, 2337; (*b*) J. S. Bradley, F. Cheng, S. J. Archibald, R. Supplit, R. Rovai, C. W. Lehmann, C. Krüger and F. Lefebvre, *Dalton Trans.*, 2003, 1846; (*c*) V. Jancik, F. Rascón-Cruz, R. Cea-Olivares and R. A. Toscano, *Chem. Commun.*, 2007, 4528; (*d*) D. A. Atwood and D. Rutherford, *Inorg. Chem.*, 1995, **34**, 4008; (*e*) H. Naka, M. Uchiyama, Y. Matsumoto, A. E. H. Wheatley, M. McPartlin, J. V. Morey and Y. Kondo, *J. Am. Chem. Soc.*, 2007, **129**, 1921; (*f*) J. Garcia-Alvarez, E. Hevia, A. R. Kennedy, J. Klett and R. E. Mulvey, *Chem. Commun.*, 2007, 2402; (*g*) D. Rutherford and D. A. Atwood, *J. Am. Chem. Soc.*, 1996, **118**, 11535.

21 (*a*) M. Veith, O. Schutt, J. Blin, S. Becker, J. Freres and V. Huch, *Z. Anorg. Allg. Chem.*, 2002, **628**, 138; (*b*) J. M. Pietryga, J. D. Gorden, C. L. B. Macdonald, A. Voigt, R. J. Wiacek and A. H. Cowley, *J. Am. Chem. Soc.*, 2001, **123**, 7713; (*c*) O. M. Kekia, C. L. Watkins, L. K. Krannich, A. L. Rheingold and L. M. Liable-Sands, *Organometallics*, 2001, **20**, 582; (*d*) T. Chivers, D. J. Eisler, C. Fedorchuk, G. Schatte, H. M. Tuononen and R. T. Boeré, *Chem. Commun.*, 2005, 3930.

22 (*a*) Z. Csok, O. Vechorkin, S. B. Harkins, R. Scopelliti and X. Hu, *J. Am. Chem. Soc.*, 2008, **130**, 8156; (*b*) P.-C. Kuo, J.-C. Chang, W.-Y. Lee, H. M. Lee and J.-H. Huang, *J. Organomet. Chem.*, 2005, **690**, 4168.

23 (*a*) O. M. Kekia, L. K. Krannich, C. L. Watkins, C. D. Incarvito and A. L. Rheingold, *Organometallics*, 2002, **21**, 5987; (*b*) E. K. Styron, C. H. Lake, C. H. Watkins and L. K. Krannich, *Organometallics*, 1998, **17**, 4319; (*c*) O. M. Kekia, C. L. Watkins, L. K. Krannich, A. L. Rheingold and L. M. Liable-Sands, *Organometallics*, 2001, **20**, 582; (*d*) C.-C. Zhou, C.-H. Hung, J.-H. Huang and T.-Y. Lee, *J. Chin. Chem. Soc.*, 2006, **53**, 1297; (*e*) D. S. Brown, A. Decken, C. A. Schnee and A. H. Cowley, *Inorg. Chem.*, 1995, **34**, 6415; (*f*) M. G. Gardiner, S. M. Lawrence and C. L. Raston, *J. Chem. Soc., Dalton Trans.*, 1996, 4163; (*g*) E. K. Styron, C. H. Lake, C. L. Watkins, L. K. Krannich, C. D. Incarvito and A. L. Rheingold, *Organometallics*, 2000, **19**, 3253; (*h*) P. B. Hitchcock, H. A. Jasim, M. F. Lappert and H. D. Williams, *Polyhedron*, 1990, **9**, 245; (*i*) M. D. B. Dillingham, J. B. Hill, B. Lee, S. J. Schauer, W. T. Pennington, G. H. Robinson and D. C. Hrncir, *J. Coord. Chem.*, 1993, **28**, 337; (*j*) S. Schulz, L. Häming, R. Herbst-Irmer, H. W. Roesky and G. M. Sheldrick, *Angew. Chem., Int. Ed. Engl.*, 1994, **33**, 969.

24 J.-P. Bezombes, B. Gehrhus, P. B. Hitchcock, M. F. Lappert and P. G. Merle, *Dalton Trans.*, 2003, 1821.

25 M. Haddad, M. Laghzaoui, R. Welter and S. Dagorne, *Organometallics*, 2009, **28**, 4584.

26 S. Milione, F. Grisi, R. Centore and A. Tuzi, *Organometallics*, 2006, **25**, 266.

27 (*a*) D. Chakraborty and E. Y. Chen, *Organometallics*, 2002, **21**, 1438; (*b*) J. Lewinski, P. Horeglad, M. Dranka and I. Justyniak, *Inorg. Chem.*, 2004, **43**, 5789.

28 (*a*) Bruker AXS, APEX2, V1.0; SADABS V2.1; SAINT+ V6.28a; SHELXTL V6.14, Bruker AXS Inc., Madison, Wisconsin, USA, 2004; (*b*) Bruker AXS, APEX2, V2010; SADABS V2008/1; SAINT+ V7.66a; SHELXTL V6.14, Bruker AXS Inc., Madison, Wisconsin, USA, 2010.

29 A. D. Becke, *J. Chem. Phys.*, 1993, **98**, 5648.

30 C. Lee, W. Yang and R. G. Parr, *Phys. Rev.*, 1988, **B37**, 78.

31 M. J. Frisch, G. W. Trucks, H. B. Schlegel, G. E. Scuseria, M. A. Robb, J. R. Cheeseman, J. A. Montgomery, Jr., T. Vreven, K. N. Kudin, J. C. Burant, J. M. Millam, S. S. Iyengar, J. Tomasi, V. Barone, B. Mennucci, M. Cossi, G. Scalmani, N. Rega, G. A. Petersson, H. Nakatsuji, M. Hada, M. Ehara, K. Toyota, R. Fukuda, J. Hasegawa, M. Ishida, T. Nakajima, Y. Honda, O. Kitao, H. Nakai, M. Klene, X. Li, J. E. Knox, H. P. Hratchian, J. B. Cross, V. Bakken, C. Adamo, J. Jaramillo, R. Gomperts, R. E. Stratmann, O. Yazyev, A. J. Austin, R. Cammi, C. Pomelli, J. Ochterski, P. Y. Ayala, K. Morokuma, G. A. Voth, P. Salvador, J. J. Dannenberg, V. G. Zakrzewski, S. Dapprich, A. D. Daniels, M. C. Strain, O. Farkas, D. K. Malick, A. D. Rabuck, K. Raghavachari, J. B. Foresman, J. V. Ortiz, Q. Cui, A. G. Baboul, S. Clifford, J. Cioslowski, B. B. Stefanov, G. Liu, A. Liashenko, P. Piskorz, I. Komaromi, R. L. Martin, D. J. Fox, T. Keith, M. A. Al-Laham, C. Y. Peng, A. Nanayakkara, M. Challacombe, P. M. W. Gill, B. G. Johnson, W. Chen, M. W. Wong, C. Gonzalez and J. A. Pople, *GAUSSIAN 03 (Revision C.02)*, Gaussian, Inc., Wallingford, CT, 2004.